Robust Photon Locking

T. Bayer, M. Wollenhaupt, C. Sarpe-Tudoran, and T. Baumert

Universität Kassel, Institut für Physik und CINSaT, Heinrich-Plett-Str. 40, D-34132 Kassel, Germany

(Received 28 August 2008; published 16 January 2009)

We experimentally demonstrate a strong-field coherent control mechanism that combines the advantages of photon locking (PL) and rapid adiabatic passage (RAP). Unlike earlier implementations of PL and RAP by pulse sequences or chirped pulses, we use shaped pulses generated by phase modulation of the spectrum of a femtosecond laser pulse with a generalized phase discontinuity. The novel control scenario is characterized by a high degree of robustness achieved via adiabatic preparation of a state of maximum coherence. Subsequent phase control allows for efficient switching among different target states. We investigate both properties by photoelectron spectroscopy on potassium atoms interacting with the intense shaped light field.

DOI: 10.1103/PhysRevLett.102.023004 PACS numbers: 32.80.Qk, 32.80.Fb, 42.50.Hz

The rapid progress of ultrafast laser science in recent decades has delivered invaluable insights into ultrafast light-induced processes at a microscopic level. Powerful methodologies have been devised to observe [1] and to control [2] molecular dynamics on their intrinsic femtosecond time scale. Recently, strategies for observation of ultrafast processes have been developed by adopting techniques known from nuclear magnetic resonance (NMR), a prime example of which is the emerging field of femtosecond 2D Fourier transform spectroscopy [3]. The concept of spin locking [4], being at the heart of liquid phase NMR and solid state nuclear quadrupole resonance [5], has been successfully transferred to the optical regime by modulation of cw laser radiation [6,7]. Photon locking (PL), as the optical analog of spin locking was termed [6], involves the initial excitation of a superposition state at maximum coherence by a preparatory laser pulse followed by a second $\pi/2$ phase shifted pulse that maintains this coherence throughout the whole interaction, i.e., locks the populations in time. With the advent of ultrashort laser pulses and the associated options for pulse shaping [8], the potential to utilize PL as an efficient tool to manipulate ultrafast molecular dynamics was studied theoretically [9–11]. Recent experimental implementations of PL based on the coherent interaction of *intense ultrashort* shaped laser pulses with quantum systems [12–14] reveal the prospects of PL to act as an efficient ultrafast quantum mechanical switch, allowing to achieve selective excitation of a preselected target channel. However, due to the nonlinearities involved in the nonperturbative light matter interaction, strong-field control scenarios [15,16] inherently suffer from their sensitivity to intensity variations potentially limiting their practical use and concealing strong-field effects by averaging over the intensity distribution within the laser focus. In PL scenarios demonstrated so far, phase control could even be inhibited by improper choice of the intensity [14,15] since the PL effectiveness crucially depends on the initial preparation of a state of maximum coherence. For practical applications it is highly desirable to devise refined strong-field control scenarios inherently *robust* to intensity variations. Enormous robustness is a salient characteristic of adiabatic control scenarios [17] which, by virtue of the adiabatic condition, become more stable with increasing intensity.

Here we present a novel control scenario that combines the advantages of adiabatic techniques in terms of robustness with the efficient switching capabilities of PL by reliable preparation of a state of maximum coherence and subsequent phase control for efficient switching. Our approach makes use of a simple pulse shape generated by the spectral phase modulation function

$$\tilde{M}(\omega) = e^{-i(\theta/2)\sigma(\omega-\delta\omega)}, \tag{1}$$

where the *signum* function σ describes a symmetric phase jump of θ spectrally shifted from the laser central frequency ω_0 by the detuning $\delta\omega$ [18]. The resulting temporal field is a double pulse sequence, as required to enable PL. Both pulses feature a time-dependent detuning being a basic prerequisite for adiabaticity. Experimentally, we studied PL on near-resonant strong-field photoionization of potassium atoms. Both, the switching efficiency associated with PL and switching robustness, were investigated by variation of the control parameters step amplitude θ and detuning $\delta\omega$ and variation of the laser intensity, respectively. Intense 795 nm, 30 fs FWHM laser pulses provided by a 1 kHz Ti:sapphire laser were phase modulated by a home-built pulse shaper [19], applying a θ-step phase mask [see Eq. (1)]. The shaped output pulses were attenuated to pulse energies of 0.6–1.4 μJ and focussed into a potassium beam. Photoelectrons released during the laser-atom interaction were detected by an energy calibrated magnetic bottle time-of-flight spectrometer. In this manner we studied energy resolved photoelectron spectra as a function of θ and $\delta\omega$. Figure 1(a) shows the $1 + 2$ resonance enhanced multiphoton excitation and ionization scheme for the interaction of shaped intense laser pulses

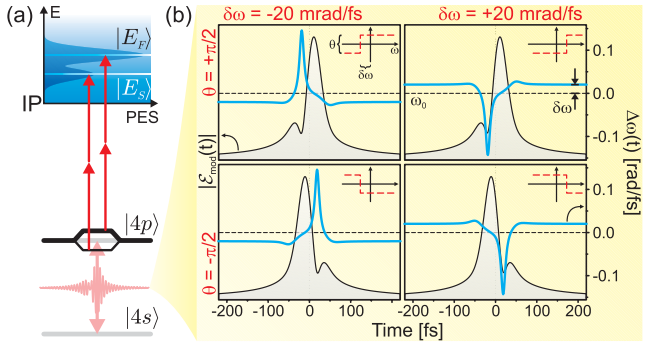

FIG. 1 (color online). (a) Excitation or ionization scheme of potassium atoms. Strong-field interaction of the shaped intense pulse with the neutral system $4s - 4p$ (faded lines) lifts the degeneracy of dressed states (black lines) which are probed simultaneously by two-photon ionization. (b) Pulse shapes resulting from θ-step modulation of a 30 fs Gaussian input pulse.

with potassium atoms. Resonant *nonperturbative* interaction of the neutral system with the laser field gives rise to dressed atomic states (black lines). The corresponding eigenenergies split up proportional to the Rabi frequency $\Omega(t)$. Simultaneous two-photon ionization maps the dressed state populations into the continuum [10,13] such that two ionization channels are observed with energies E_S and E_F separated by the dressed state energy splitting. Switching between these two channels reveals selective population of dressed states (SPODS) [10,12].

To clarify the significance of the two modulation parameters θ and $\delta\omega$, the temporal structure of the modulated electric field $\mathcal{E}_{\mathrm{mod}}(t)$ is analyzed. Starting with the unmodulated temporal pulse envelope $\mathcal{E}(t)$ and its Fourier transform $\tilde{\mathcal{E}}(\omega)$, we apply the spectral modulation function $\tilde{M}(\omega)$ defined in Eq. (1) to obtain the modulated spectrum $\tilde{\mathcal{E}}_{\mathrm{mod}}(\omega) = \tilde{\mathcal{E}}(\omega)\tilde{M}(\omega)$. The modulated *temporal* electric field is the convolution of the input field $\mathcal{E}(t)$ with the temporal modulation function $M(t)$, i.e., $\mathcal{E}_{\mathrm{mod}}(t) = \mathcal{E}(t) \star M(t)$. The inverse Fourier transform of Eq. (1) yields $M(t) = \cos(\theta/2)\delta(t) + \sin(\theta/2)e^{i\delta\omega t}/(\pi t)$, where $\delta(t)$ describes the Dirac-delta function, implying

$$\mathcal{E}_{\mathrm{mod}}(t) = \cos(\theta/2)\mathcal{E}(t) + \sin(\theta/2)\mathcal{E}(t) \star \frac{e^{i\delta\omega t}}{\pi t}. \qquad (2)$$

Equation (2) shows that the modulated field of any input field is a linear superposition of the unmodulated field and the complex field $\mathcal{E}_c(t) = \mathcal{E}(t) \star e^{i\delta\omega t}/(\pi t)$. By tuning the step amplitude θ, we control their relative contributions via the factors $\cos(\theta/2)$ and $\sin(\theta/2)$ as illustrated in Fig. 1(b). For $\theta = +\pi/2$ (upper row), destructive interference of $\mathcal{E}(t)$ and $\mathcal{E}_c(t)$ at some time $t < 0$ leads to the formation of a weak prepulse followed by an intense pulse. Altering the sign of θ (lower row) results in a time reversed copy of the modulated pulse. Solid lines represent the instantaneous detuning $\Delta\omega(t)$, that is the difference between the instantaneous frequency $\omega(t)$ and the laser central frequency ω_0. In the wings of the pulse, the spectral shift $\delta\omega$ of the θ step induces a constant detuning of the carrier, i.e., $\Delta\omega = \delta\omega$. The distinct peak of $\Delta\omega$ around $t = 0$ is reminiscent of a π jump in the temporal phase of the modulated field. Figure 1(b) indicates that both parameters θ and $\delta\omega$ affect the modulated pulse shape (almost) independently from one another.

The experimental results on switching efficiency (Fig. 2) demonstrate highly selective switching between the population of the upper and lower dressed state via PL controlled by the parameters $\delta\omega$ and θ. Figure 2(a) shows photoelectron spectra for variation of the detuning $\delta\omega$ for a given value of $\theta = \pi$ obtained by scanning the π-step frequency across the two potassium fine structure resonances $\omega_{4p_{1/2}} = 2.446$ rad/fs and $\omega_{4p_{3/2}} = 2.457$ rad/fs. At a pulse energy of 1.0 μJ the energies of the two ionization channels are $E_S = 0.22$ eV and $E_F = 0.45$ eV [black arrows in Fig. 2(a)]. This amounts to an energy splitting of 230 meV corresponding to a laser intensity of 2.2×10^{11} W/cm^2 in the interaction region. Results from numerical simulations performed by solving the time-dependent Schrödinger equation for neutral potassium interacting nonperturbatively with the modulated pulse and perturbatively coupled to the continuum show excellent agreement with the experimental results [Fig. 2(a)]. Both results reveal that for $\omega_{\mathrm{step}} < \omega_{4p_{1/2}}$ the lower dressed state is populated with high selectivity and mapped into the lower channel E_S. Beyond the $4p_{3/2}$ resonance, i.e., for $\omega_{\mathrm{step}} > \omega_{4p_{3/2}}$ photoelectrons switch to the upper channel E_F indicating selective population of the upper dressed

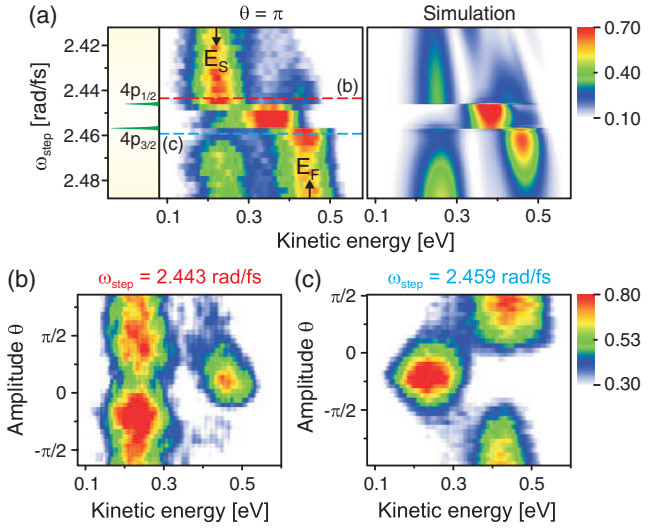

FIG. 2 (color online). Experimental evidence of switching efficiency. (a) Energy resolved photoelectron spectra measured for fixed amplitude $\theta = \pi$ and the step frequency scanned across the fine structure resonances $4p_{1/2}$ and $4p_{3/2}$ (left panel). (b) and (c) spectra measured upon variation of θ at two selected step frequencies [upper and lower dashed lines in (a)].

state. In the intermediate region when $\omega_{4p_{1/2}} < \omega_{\text{step}} < \omega_{4p_{3/2}}$, a third ionization channel between the two others is observed. This channel, which cancels the effect of power broadening, is due to a third dressed state, arising from the fine structure splitting of the $4p$ bare state. Switching by variation of θ is demonstrated in Figs. 2(b) and 2(c) for two fixed step detunings close to the $4p_{1/2}$ and $4p_{3/2}$ resonances. In these measurements the step amplitude is scanned from $\theta = -\pi$ to $+\pi$. Photoelectron spectra measured at a step frequency below the $4p_{1/2}$ resonance at $\omega_{\text{step}} = 2.443$ rad/fs [upper dashed line in Fig. 2(a)] are shown in Fig. 2(b). For $\theta < 0$ exclusively low energetic photoelectrons are observed, indicative to selective population of the lower dressed state. From about $\theta = 0$ to $\pi/4$, however, the photoelectrons switch to higher energies indicating selective population of the upper dressed state. For large positive values of θ, the photoelectrons switch back to E_S. A mirror image of these results [see Fig. 2(c)] is observed when the step frequency is shifted slightly above the $4p_{3/2}$ resonance $\omega_{\text{step}} = 2.459$ rad/fs [lower dashed line in Fig. 2(a)]. Here, for $\theta > 0$, the upper dressed state is selectively populated, which is visible by the exclusive detection of high energetic photoelectrons. The photoelectron spectrum changes at $\theta \approx 0$ such that only slow electrons are observed, indicative to selective population of the lower dressed state. At $\theta \approx -\pi/2$ the photoelectrons switch back to agree with the results presented in Fig. 2(a) at $\theta = \pi$. Our results so far show efficient switching between two target states with high selectivity by PL. Both control parameters $\delta\omega$ and θ acted as independent toggle switches to selectively populate a single dressed state.

In order to assess the *robustness* of our control scenario we repeated the π-step scan presented in Fig. 2(a) for pulse energies ranging from 0.6 μJ to 1.4 μJ. For data reduction, the observed spectra are mapped into the photoelectron contrast $C = (F - S)/(F + S)$, where S and F denote the integrated photoelectron yield of the corresponding target channel (cf. Fig. 3). The insets in Fig. 3 show the observed photoelectron spectra for two selected step frequencies representing the regions above and below the atomic resonances [Fig. 2(a)]. The *shape* of the spectra is essentially unaffected by variation of the pulse energy, i.e., robust with respect to intensity variations. This observation applies to all step frequencies ω_{step} as indicated by the contrast curves. Moreover, the curves converge with increasing pulse energy pointing towards adiabatic time evolution during the interaction process. As demonstrated previously [14], in PL a variation of the intensity by a factor of about 1.5 suffices to change the contrast from $C = 0.5$ to 0, whereas in the rapid adiabatic passage (RAP) case the contrast of $C = 0.3$ remains stable upon an intensity increase by the same amount. Comparison of the intensity dependence in the novel PL scenario depicted in the left inset to Fig. 3 ($C = 0.4$) to the previous results

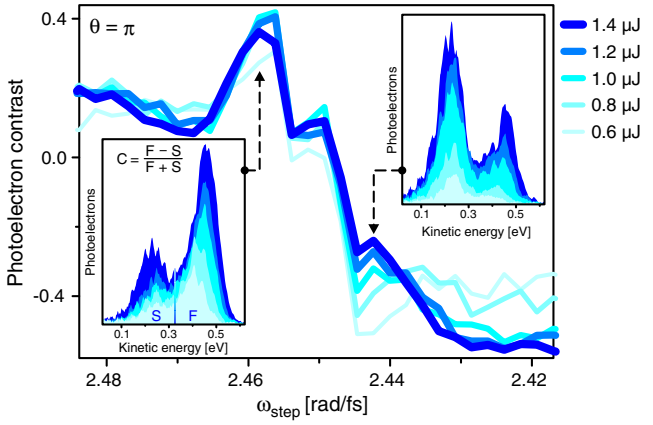

FIG. 3 (color online). Experimental demonstration of switching robustness. Photoelectron contrast C from π-step frequency scans for various pulse energies. The insets show photoelectron spectra at the two distinct step frequencies marked in Fig. 2(a). The contrast curves are similar for all intensities approximating the curve measured at the highest intensity.

reveals a high degree of robustness keeping up with that of RAP.

Finally, we give an illustrative picture of the physical mechanisms at play. To this end, we consider a model consisting of a single neutral transition $4s \leftarrow 4p$, resonantly driven by the shaped pulse. Results from numerical simulations are depicted in Fig. 4 in terms of a two-dimensional quantum control map [14,20] for the photoelectron contrast C depending on $\delta\omega$ and θ. The insets show the temporal population dynamics of both the neutral bare and dressed state system. The symmetry of the map reflects the above finding [see Fig. 1(b)] that $\delta\omega$ and θ act independently on the shape of the modulated electric field. This results in two essentially independent physical mechanisms controlling the light matter interaction. In view of the bare states, the population dynamics are very similar in all cases strongly resembling RAP. The first pulse *adiabatically* guides the system into a superposition state of maximum coherence in virtue of both the detuning and the smooth onset of the field. Because of adiabatic following, the system always arrives at the maximum coherence state in the PL configuration ensuring dressed state selectivity (in contrast, traditional PL requires a $\pi/2$ phase jump for selectivity). Consequently, the bare state populations are frozen throughout the most intense part of the pulse. The essential physical mechanism is seen in the dressed state system, whose dynamics is decomposed into three stages. Initially, the equal population of dressed states is lifted due to the detuning of the laser field. The lower dressed state is favored for $\delta\omega < 0$ [cf. Figs. 4(a) and 4(c)] and vice versa [cf. Figs. 4(b) and 4(d)]. Around $t = 0$ the dressed state populations are switched by the π jump in the optical phase of the modulated field. The final stage is characterized by multiphoton ionization *mapping* the dressed state populations onto the ionic target channels.

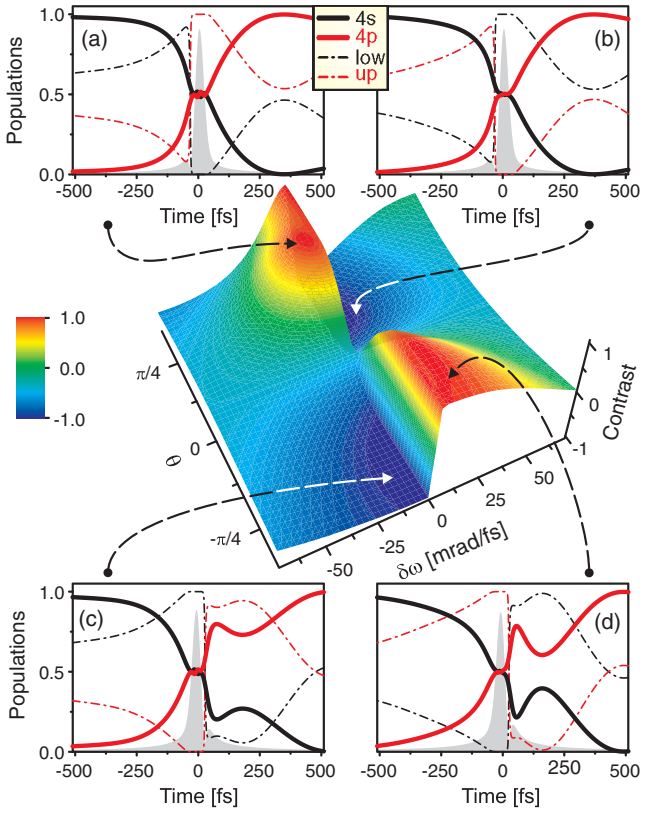

FIG. 4 (color online). Simulated quantum control map of the photoelectron contrast C as a function of the control parameters θ and $\delta\omega$. The four graphs illustrate the temporal population dynamics of both the neutral bare (bold solid lines) and dressed (dashed-dotted lines) state system in the four quadrants of the map. Lower states are depicted in black.

Since this nonlinear process takes place predominantly during the most intense part of the field, i.e., either before or after switching has occurred, the step amplitude θ determines whether the initially populated dressed state or its counterpart after inversion of the dressed state population is probed. This scenario provides high efficiency and inherent robustness and, moreover, features a high degree of flexibility since either control parameter θ and $\delta\omega$ is independently able to manipulate the course and the outcome of the population flow to the target channels.

In summary, we report on adiabatic and hence robust realizations of PL. Robust PL is a powerful tool for nonperturbative coherent control by intense shaped femtosecond laser pulses based on the advancement of well-established NMR techniques. We demonstrated in a resonant multiphoton scenario the capability of our scheme to switch among different excitation target channels with high efficiency and flexibility reminiscent of a toggle switch. Because this scenario combines the advantages of robust adiabatic state preparation with ultrafast and efficient switching by PL, it provides huge potential for strong-field applications in ultrafast spectroscopy, coherent control and quantum information processing.

Financial support by the Deutsche Forschungsgemeinschaft DFG is gratefully acknowledged.

[1] A. Zewail, J. Phys. Chem. A **104**, 5660 (2000).
[2] T. Baumert *et al.*, in *Advances in Chemical Physics* (Wiley, New York, 1997); S. Rice and M. Zhao, *Optical Control of Molecular Dynamics* (Wiley, New York, 2000); M. Shapiro and P. Brumer, *Principles of the Quantum Control of Molecular Processes* (Wiley, New York, 2003); H. Rabitz *et al.*, Science **288**, 824 (2000); R. Levis and H. Rabitz, J. Phys. Chem. A **106**, 6427 (2002); M. Dantus and V. Lozovoy, Chem. Rev. **104**, 1813 (2004); M. Wollenhaupt *et al.*, Annu. Rev. Phys. Chem. **56**, 25 (2005); T. Brixner *et al.*, in *Femtosecond Laser Spectroscopy* (Springer, New York, 2005); D. Tannor, *Introduction to Quantum Mechanics* (University Science Books, Sausalito, 2006); Special issue on Coherent Control, edited by H. Fielding *et al.* [J. Phys. B **41**, (2008)].
[3] S. Mukamel, Annu. Rev. Phys. Chem. **51**, 691 (2000); D. Jonas, Annu. Rev. Phys. Chem. **54**, 425 (2003).
[4] S. Hartmann and E. Hahn, Phys. Rev. **128**, 2042 (1962).
[5] *Encyclopedia of Nuclear Magnetic Resonance*, edited by D. Grant and R. Harris (Wiley, New York, 2002).
[6] E. Sleva *et al.*, J. Opt. Soc. Am. B **3**, 483 (1986).
[7] Y. Bai *et al.*, Phys. Rev. Lett. **55**, 1277 (1985).
[8] A. Weiner, Rev. Sci. Instrum. **71**, 1929 (2000); M. Wollenhaupt *et al.*, in *Springer Handbook of Lasers and Optics* (Springer, New York, 2007), Chap. 12.
[9] R. Kosloff *et al.*, Phys. Rev. Lett. **69**, 2172 (1992); D. Tannor *et al.*, Faraday Discuss. Chem. Soc. **113**, 365 (1999).
[10] M. Wollenhaupt *et al.*, Chem. Phys. Lett. **419**, 184 (2006).
[11] M. Wollenhaupt and T. Baumert, J. Photochem. Photobiol. A **180**, 248 (2006).
[12] M. Wollenhaupt *et al.*, J. Opt. B **7**, S270 (2005).
[13] M. Wollenhaupt *et al.*, Phys. Rev. A **73**, 063409 (2006).
[14] T. Bayer *et al.*, J. Phys. B **41**, 074007 (2008).
[15] M. Wollenhaupt *et al.*, Phys. Rev. A **68**, 015401 (2003).
[16] N. Dudovich *et al.*, Phys. Rev. Lett. **94**, 083002 (2005); C. Trallero-Herrero *et al.*, Phys. Rev. Lett. **96**, 063603 (2006).
[17] U. Gaubatz *et al.*, Chem. Phys. Lett. **149**, 463 (1988); N. Vitanov *et al.*, Annu. Rev. Phys. Chem. **52**, 763 (2001); M. Wollenhaupt *et al.*, Appl. Phys. B **82**, 183 (2006); E. Shapiro *et al.*, Phys. Rev. Lett. **101**, 023601 (2008).
[18] D. Meshulach and Y. Silberberg, Phys. Rev. A **60**, 1287 (1999); M. Renard *et al.*, Opt. Express **12**, 473 (2004); A. Präkelt *et al.*, Phys. Rev. A **70**, 063407 (2004); P. Panek and A. Becker, Phys. Rev. A **74**, 023408 (2006).
[19] A. Präkelt *et al.*, Rev. Sci. Instrum. **74**, 4950 (2003).
[20] H. Rabitz *et al.*, Science **303**, 1998 (2004); M. Wollenhaupt *et al.*, J. Mod. Opt. **52**, 2187 (2005).